Differential Amplitude Pulse-Position Modulation for Indoor Wireless Optical Communications

Ubolthip Sethakaset

Department of Electrical and Computer Engineering, University of Victoria, P.O. Box 3055 STN CSC,
Victoria, BC, Canada V8W 3P6
Email: usethaka@ece.uvic.ca

T. Aaron Gulliver

Department of Electrical and Computer Engineering, University of Victoria, P.O. Box 3055 STN CSC,
Victoria, BC, Canada V8W 3P6
Email: agullive@ece.uvic.ca

We propose a novel differential amplitude pulse-position modulation (DAPPM) for indoor optical wireless communications. DAPPM yields advantages over PPM, DPPM, and DH-PIM$_\alpha$ in terms of bandwidth requirements, capacity, and peak-to-average power ratio (PAPR). The performance of a DAPPM system with an unequalized receiver is examined over nondispersive and dispersive channels. DAPPM can provide better bandwidth and/or power efficiency than PAM, PPM, DPPM, and DH-PIM$_\alpha$ depending on the number of amplitude levels A and the maximum length L of a symbol. We also show that, given the same maximum length, DAPPM has better bandwidth efficiency but requires about 1 dB and 1.5 dB more power than PPM and DPPM, respectively, at high bit rates over a dispersive channel. Conversely, DAPPM requires less power than DH-PIM$_2$. When the number of bits per symbol is the same, PAM requires more power, and DH-PIM$_2$ less power, than DAPPM. Finally, it is shown that the performance of DAPPM can be improved with MLSD, chip-rate DFE, and multichip-rate DFE.

Keywords and phrases: differential amplitude pulse-position modulation, optical wireless communications, intensity modulation and direct detection, decision-feedback equalization.

1. INTRODUCTION

Recently, the need to access wireless local area networks from portable personal computers and mobile devices has grown rapidly. Many of these networks have been designed to support multimedia with high data rates, thus the systems require a large bandwidth. Since radio communication systems have limited available bandwidth, a proposal to use indoor optical wireless communications has received wide interest [1, 2]. The major advantages of optical systems are low-cost optical devices and virtually unlimited bandwidth.

A nondirected link, exploiting the light-reflection characteristics for transmitting data to a receiver, is considered to be the most suitable for optical wireless systems in an indoor environment [2]. This link can be categorized as either line-of-sight (LOS) or diffuse. A diffuse link is preferable because there is no alignment requirement and it is more robust

to shadowing. However, a diffuse link is more susceptible to corruption by ambient light noise, high signal attenuation, and intersymbol interference caused by multipath dispersion. Thus, a diffuse link needs more transmitted power than an LOS link. A well-approximated indoor free-space optical link with the effects of multipath dispersion was presented in [3]. Nevertheless, the average optical transmitter power level is constrained by concerns about power consumption and eye safety. Furthermore, high capacitance in a large-area photodetector limits the receiver bandwidth. Consequently, a power-efficient and bandwidth-efficient modulation scheme is desirable in an indoor optical wireless channel.

Normally, an optical wireless system adopts a simple baseband modulation scheme such as on-off keying (OOK) or pulse-position modulation (PPM). To provide more power efficiency, a number of modulation techniques have been proposed which vary the number of chips per symbol, for example, digital pulse-interval modulation (DPIM) [4, 5, 6], differential pulse-position modulation (DPPM) which can be considered as DPIM (with no guard slot) [5, 7], and dual header pulse-interval modulation (DH-PIM$_\alpha$) [8, 9].

However, these techniques require more bandwidth as the maximum symbol length increases. Multilevel modulation schemes were introduced in [10, 11] to achieve better bandwidth efficiency at the cost of higher power requirements.

In this paper, a novel hybrid modulation technique called differential amplitude pulse-position modulation (DAPPM) is proposed. DAPPM is a combination of pulse-amplitude modulation (PAM) and DPPM. The performance is investigated for different types of detection, for example, hard-decision, maximum-likelihood sequence detection (MLSD), and a zero-forcing decision-feedback equalizer (ZF-DFE). The remainder of this paper is organized as follows. In Section 2, the optical wireless channel is presented. In Section 3, the symbol structure and properties of DAPPM, for example, peak-to-average power ratio (PAPR), bandwidth requirements, and capacity are discussed. The power spectral density is also derived and compared to that of other modulation schemes. In Section 4, the probability of error is analyzed for DAPPM with hard-decision detection on nondispersive and dispersive channels. In Section 5, the performance improvement with an MLSD receiver is examined, and the performance with a ZF-DFE is investigated in Section 6. Finally, some conclusions are given in Section 7.

2. THE INDOOR OPTICAL WIRELESS CHANNEL

When an infrared signal is incident on an ideal Lambertian reflector, it will radiate in all directions. An optical wireless communication system exploits this property to send and receive data in an indoor environment. The features of a room, for example, walls, ceiling, and office materials, can be approximated as an ideal Lambertian reflector [1]. The nondirected optical wireless link (the most practical link) has been investigated and simulated in [3, 12]. Normally, an optical wireless system adopts an intensity modulation and direct detection technique (IM/DD) because of its simple implementation. In an optical system, an optical emitter and a large-area photodetector are used as the transmitter and receiver, respectively. The output current $y(t)$ generated by the photodetector can be written as

$$y(t) = Rh(t) * x(t) + n(t), \qquad (1)$$

where $*$ denotes convolution, R is the photodetector responsivity (in A/W), and $h(t)$ is the channel impulse response. In an optical wireless link, the noise $n(t)$, which is usually the ambient light, can be modeled as white Gaussian noise [2]. Since the transmitted signal $x(t)$ represents infrared power, it cannot be negative and must satisfy eye safety regulations [2], that is,

$$x(t) \geq 0, \qquad \lim_{T \to \infty} \frac{1}{2T} \int_{-T}^{T} x(t)dt \leq P_{\text{avg}}, \qquad (2)$$

where P_{avg} is the average optical-power constraint of the light emitter. The advantage of using IM/DD is its spatial diversity. An optical system with a large square-law detector operates on a short wavelength which can mitigate the multipath fading. Since the room configuration does not change, the
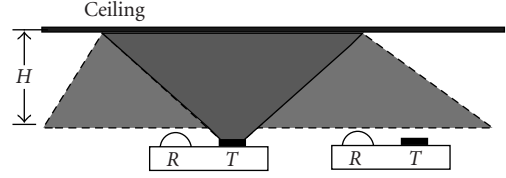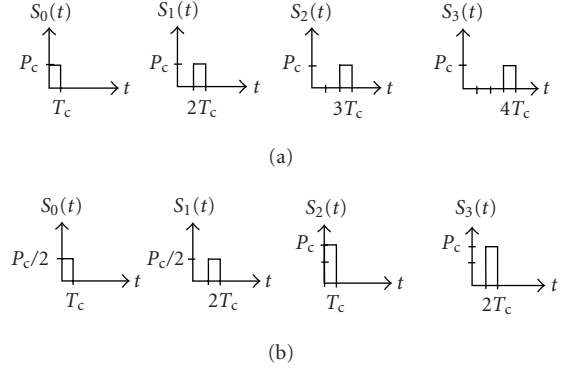

FIGURE 1: A ceiling-bounce optical wireless model.

(a)

(b)

FIGURE 2: The symbol structure for $M = 2$ bits/symbol with (a) DPPM ($L = 4$) and (b) DAPPM ($A = 2, L = 2$).

infrared wireless link with IM/DD could be considered as a linear time-invariant channel.

The ceiling-bounce model, as shown in Figure 1, developed by Carruthers and Kahn in [3], is chosen as the channel model in this paper since it is the most practical and represents the multipath dispersion of an indoor wireless optical channel accurately. The channel model is characterized by two parameters, rms delay spread D_{rms} and optical path loss $H(0)$, which cause intersymbol interference and signal attenuation, respectively. The impulse response of an optical wireless link can be represented as

$$h(t) = H(0) \frac{6a^6}{(t+a)^7} u(t), \qquad (3)$$

where $u(t)$ is the unit step function and a depends on the room size and the transmitter and receiver position. If the transmitter and receiver are colocated, $a = 2H/c$ where H is the height of the ceiling above the transmitter and the receiver and c is the speed of light. The parameter a is related to the rms delay spread D_{rms} by

$$D_{\text{rms}} = \frac{a}{12}\sqrt{\frac{13}{11}}. \qquad (4)$$

3. DIFFERENTIAL AMPLITUDE PULSE-POSITION MODULATION

DAPPM is a combination of PAM and DPPM. Therefore the symbol length and pulse amplitude are varied according to the information being transmitted. A block of $M = \log_2(A \times L)$

Table 1: Mapping of 3-bit OOK words into PPM, DPPM, DH-PIM$_2$, and DAPPM symbols.

OOK	PPM ($L = 8$)	DPPM ($L = 8$)	DH-PIM$_2$ ($L = 8$)	DAPPM ($A = 2, L = 4$)	DAPPM ($A = 4, L = 2$)
000	10000000	1	100	1	1
001	01000000	01	1000	01	01
010	00100000	001	10000	001	2
011	00010000	0001	100000	0001	02
100	00001000	00001	110000	2	3
101	00000100	000001	11000	02	03
110	00000010	0000001	1100	002	4
111	00000001	00000001	110	0002	04

Table 2: PAPR, bandwidth requirements, and capacity of PPM, DPPM, DH-PIM$_\alpha$, and DAPPM where M represents the number of bits/symbol.

Modulation scheme	PPM	DPPM	DH-PIM$_\alpha$	DAPPM
PAPR	2^M	$\dfrac{2^M + 1}{2}$	$\dfrac{2(2^{M-1} + 2\alpha + 1)}{3\alpha}$	$\dfrac{2^M + A}{(A + 1)}$
Bandwidth requirement (Hz)	$\dfrac{2^M R_b}{M}$	$\dfrac{(2^M + 1)R_b}{2M}$	$\dfrac{(2^{M-1} + 2\alpha + 1)R_b}{2M}$	$\dfrac{(2^M + A)R_b}{2MA}$
Capacity	M	$\dfrac{2M2^M}{(2^M + 1)}$	$\dfrac{2M2^M}{(2^{M-1} + 2\alpha + 1)}$	$\dfrac{2MA2^M}{(2^M + A)}$

input bits is mapped to one of 2^M distinct waveforms, each of which has one "on" chip which is used to indicate the end of a symbol. The amplitude of the "on" chip is selected from the set $\{1, 2, \ldots, A\}$ and the length of a DAPPM symbol is selected from the set $\{1, 2, \ldots, L\}$. Alternatively, the DAPPM encoder transforms an information symbol into a chip sequence according to a DAPPM coding rule such as the one shown in Table 1. The transmitted DAPPM signal is then

$$x(t) = \sum_{k=-\infty}^{\infty} \left(\frac{P_c}{A}\right) b_k p(t - kT_c), \tag{5}$$

where $b_k \in \{0, 1, \ldots, A\}$, $p(t)$ is a unit-amplitude rectangular pulse shape with a duration of one chip (T_c), and P_c is the peak transmit power. The PAPR of DAPPM is then

$$\text{PAPR} = \frac{P_c}{P_{\text{avg}}} = \frac{A(L + 1)}{(A + 1)}. \tag{6}$$

A chip duration is $T_c = 2M/(L + 1)R_b$, where R_b represents the data bit rate. Therefore, the required bandwidth of DAPPM is given by

$$W = \frac{(L + 1)R_b}{2M}. \tag{7}$$

The average bit rate R_b is $M/(L_{\text{avg}}T_c)$ [8]. The average length of a DAPPM symbol is $L_{\text{avg}} = (L + 1)/2$, so the average bit rate is $R_b = 2M/((L + 1)T_c)$. The transmission capacity is defined as the average bit rate of a modulation scheme normalized to that of OOK. In other words, the capacity is the number of bits which can be transmitted during the time

required to transmit M bits for OOK. In this paper, we compare the information capacity of PPM, DPPM, DH-PIM$_\alpha$, and DAPPM assuming that they have the same chip duration. Hence, the transmission capacity of DAPPM is

$$\text{Capacity} = \frac{2M(A \times L)}{(L + 1)}. \tag{8}$$

The properties of PPM, DPPM, DH-PIM$_\alpha$, and DAPPM are summarized in Table 2. Compared to the other modulation schemes, DAPPM provides better bandwidth efficiency, higher transmission capacity, and a lower PAPR. Figure 3 shows that the capacity of DAPPM approaches $2A$ times and A times that of PPM and DPPM, respectively, as the number of bits/symbol increases. The capacity of DH-PIM$_2$ is about the same as DAPPM ($A = 2$).

Next the power spectral density of DAPPM is derived. From (5), $x(t)$ can be viewed as a cyclostationary process, [13, 14], with a power spectral density (PSD) given by $S(f) = (1/T_c)|P(f)|^2 S_b(f)$. For a rectangular pulse $p(t)$, $|P(f)|^2 = T_c^2 \text{sinc}^2(fT_c)$. $S_b(f)$ is the discrete-time Fourier transform of the chip autocorrelation function R_k, which is defined by $R_{n-m} = E[b_n b_m]$. The autocorrelation of the chip sequence R_k is

$$R_0 = \frac{(A + 1)(2A + 1)}{3(L + 1)},$$

$$R_k = \begin{cases} \dfrac{(A + 1)^2 (L + 1)^{k-2}}{2L^k}, & 1 \leq k \leq L, \\ \dfrac{1}{AL} \sum_{i=1}^{L} R_{k-i}, & k > L. \end{cases} \tag{9}$$
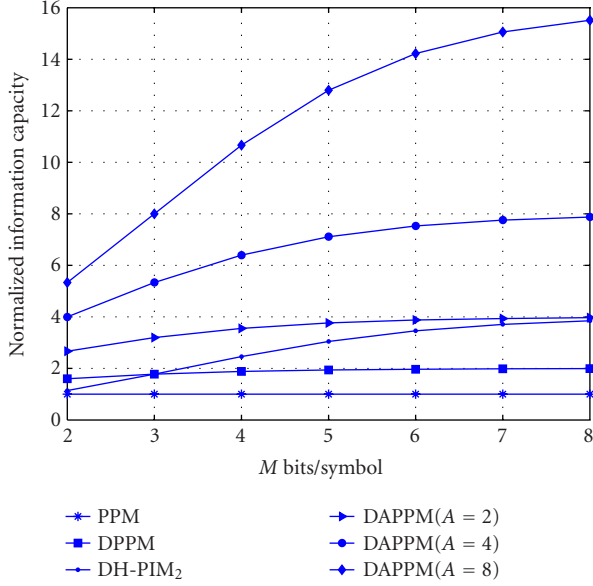
FIGURE 3: The capacity of PPM, DPPM, DH-PIM$_2$, and DAPPM normalized to the capacity of OOK (M bits/symbol).

FIGURE 4: The power spectral density of OOK, PPM, DPPM, DH-PIM$_2$, and DAPPM with the discrete spectral portion omitted when the number of bits/symbol is 4. All curves represent the same average transmitted optical power with a rectangular pulse shape.

R_k converges to $E[b]^2$ where $E[b] = (A+1)/(A(L+1))$, as k increases, so the continuous and discrete components of the PSD can be approximated as

$$S_c(f) \approx \sum_{k=-5L}^{5L} \left[R_k - E[b]^2 \right] \exp\left(-j2\pi k f T_c \right),$$

$$S_d(f) = \frac{E[b]^2}{T_c} \sum_{k=-\infty}^{\infty} \delta\left(f - \frac{k}{T_c} \right), \quad (10)$$

respectively. A comparison of the power spectral density of DAPPM with those of other modulation schemes is illustrated in Figure 4. Given the same number of bits/symbol, the PSD of DAPPM is similar to those of DPPM and DH-PIM$_2$. In addition, DAPPM requires less bandwidth but it is more susceptible to baseline wander [5] because the PSD of DAPPM has a larger DC component.

4.   ERROR PROBABILITY ANALYSIS OF DAPPM WITH A HARD-DECISION DETECTOR

A block diagram of the DAPPM transmitter is shown in Figure 5a. Each block of M input bits is converted into one of the $2^M = A \times L$ possible symbols. Each chip b_k is input to a transmit filter with a unit-amplitude rectangular pulse shape and multiplied by P_c/A. The transmitted signal is corrupted by white Gaussian noise $n(t)$. The received signal passes through a receive filter $r(t) = p(-t)$ matched to the transmitted pulse. The output of the receive filter is sampled and converted into a chip sequence by comparing the samples with an optimal threshold as shown in Figure 5b. The filter output r_k is compared to the optimal detection thresholds $\{\theta_1, \ldots, \theta_A\}$ (which are relative to P_c) to estimate the trans-
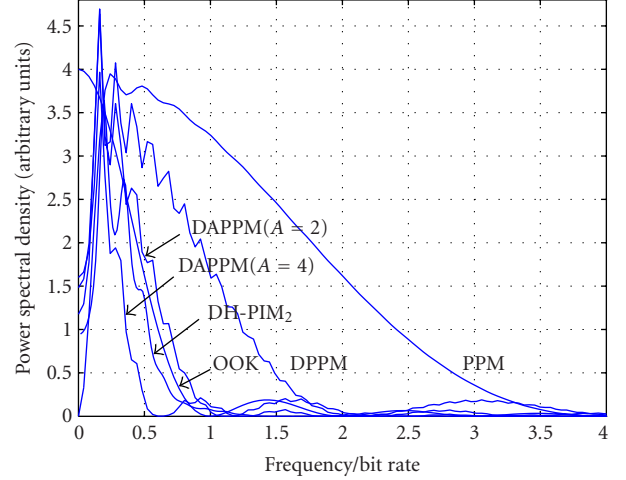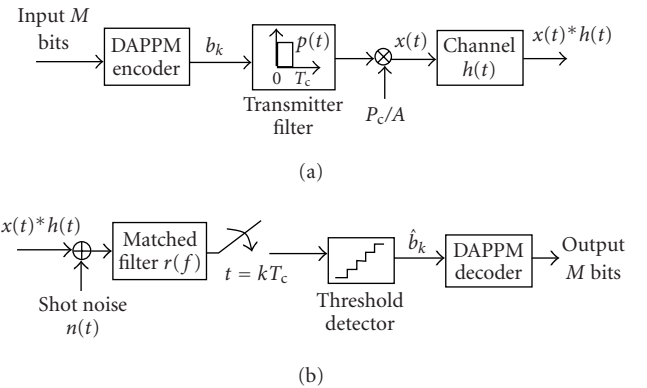

FIGURE 5: (a) Block diagram of a DAPPM transmitter. The data bit sequence (a_k) is transformed to the chip sequence (b_k) according to the DAPPM coding rule. An "on" chip induces the generation of a rectangular pulse $p(t)$ with amplitude $(b_k P_c)/A$. The resulting optical signal $x(t)$ is transmitted through a channel with impulse response $h(t)$. (b) Block diagram of an unequalized hard-decision DAPPM receiver comprised of a receive filter $r(t) = p(-t)$, matched to the transmitted pulse shape, and an optimum threshold detector.

mitted chip b_k as

$$\hat{b}_k = \begin{cases} 0 & \text{iff } r_k < \theta_1, \\ i & \text{iff } \theta_i \leq r_k < \theta_{i+1}, \ i = 1, 2, \ldots, A-1, \\ A & \text{iff } r_k \geq \theta_A. \end{cases} \quad (11)$$

The equivalent discrete-time impulse response of the system can be written as

$$f_k = f(t)|_{t=kT_c} = \frac{P_c}{A} p(t) * h(t) * r(t)|_{t=kT_c}. \quad (12)$$

In an optical wireless system, we compare the performance of modulation schemes by evaluating the power penalty, which is the average power requirement normalized by the average power required to transmit the data over a nondispersive channel using OOK modulation at the same error probability. The power penalty can be calculated as

$$\text{Power penalty} = \frac{P(\text{BER}, h(t), N_0, \text{Modulation Scheme})}{P(\text{BER}, \delta(t), N_0, \text{OOK})}, \tag{13}$$

where the bit error rate for OOK is

$$\text{BER}_{\text{OOK}} = Q\left(\frac{RP_{\text{avg}}}{\sqrt{R_b N_0}}\right), \tag{14}$$

and $P(\text{BER}, h(t), N_0, \text{Modulation Scheme})$ represents the average power required to achieve a specific error probability with a modulation scheme over a channel with impulse response $h(t)$ and white Gaussian noise with two-sided noise power spectral density N_0. In this paper, we only consider the effects of noise and multipath dispersion, so it is assumed that there is no path loss, $H(0) = 1$, and the photodetector responsivity is $R = 1$.

4.1. Nondispersive channels

We first consider the performance of DAPPM over a nondispersive channel, that is, $h(t) = \delta(t)$. The input symbols are assumed to be independent, and identically distributed. Let p_0 denote the probability of receiving an "off" chip, and p_A the probability of receiving a pulse with nonzero amplitude. Then the probability of chip error is given by

$$P_{\text{ce}} = p_0 Q\left\{\frac{\theta_1 P_c}{A\sqrt{N_0 W}}\right\}$$
$$+ p_A \sum_{i=1}^{A-1} \left(Q\left\{\frac{(i - \theta_i)P_c}{A\sqrt{N_0 W}}\right\} + Q\left\{\frac{(\theta_{(i+1)} - i)P_c}{A\sqrt{N_0 W}}\right\}\right) \tag{15}$$
$$+ p_A Q\left\{\frac{(A - \theta_A)P_c}{A\sqrt{N_0 W}}\right\}.$$

Similar to DPPM, the "on" chip indicates a symbol boundary. Therefore, the DAPPM receiver is simpler than that for PPM since symbol synchronization is not required (but chip synchronization is still needed). However, since there is no fixed symbol boundary, a single chip error affects not only the current symbol, but also the next symbol. Therefore, we will compare the performance of DAPPM to other types of modulation in terms of their packet error rates. To transmit a D-bit packet, the average DAPPM chip sequence length $\bar{N}$ is $(DL_{\text{avg}})/M$ and the packet error rate can be approximated by [9]

$$\text{PER} = 1 - (1 - P_{\text{ce}})^{L_{\text{avg}}D/M} \approx \frac{L_{\text{avg}}DP_{\text{ce}}}{M}. \tag{16}$$
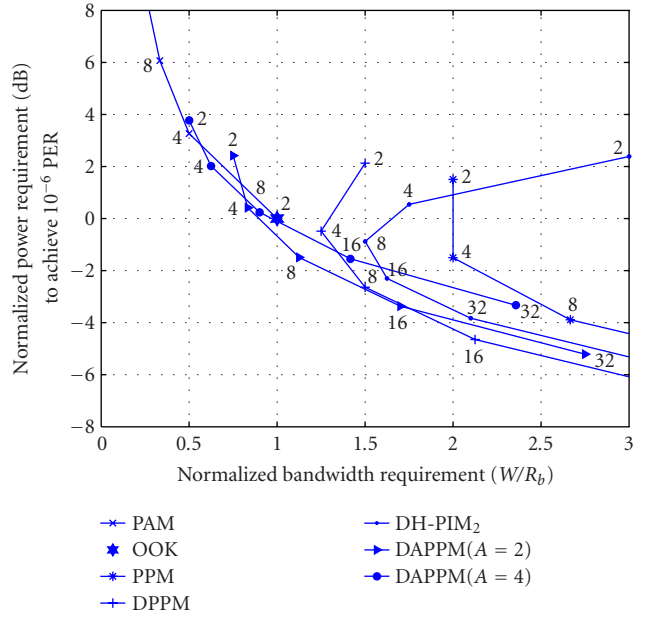

FIGURE 6: The normalized optical power and bandwidth required for OOK, PAM, PPM, DPPM, DH-PIM$_2$ and DAPPM over a nondispersive channel. Each point of DAPPM represents the maximum symbol length (L). For other modulation schemes, each point represents the number of possible symbols (2^M).

Throughout this paper, power requirements are normalized to the power required to send 1000-bit packets using OOK at an average packet error rate of 10^{-6}. Figure 6 shows the average optical power and bandwidth requirements of OOK, PAM, PPM, DPPM, DH-PIM$_2$, and DAPPM. DAPPM can give better bandwidth and/or power efficiency than PAM, PPM, DPPM, and DH-PIM$_2$ depending on the number of amplitude levels (A) and the maximum length (L) of a symbol. Given the same power penalty as PPM ($L = 4$) (which has been adopted as an IrDA standard [15]), DAPPM ($A = 2$, $L = 8$) and DAPPM ($A = 4$, $L = 16$) provide better bandwidth efficiency, capacity, and PAPR. In particular, DAPPM ($A = 2, L = 16$) yields better power efficiency and double the capacity of DPPM ($L = 8$), albeit at a slightly lower bandwidth efficiency.

4.2. Dispersive channels

In this section, we consider the performance of DAPPM over a dispersive channel which has an impulse response given in (3) and causes intersymbol interference. Thus, when the bit rate increases, the performance of the system will be degraded. Here, we focus our attention on the effects of ISI caused by multipath dispersion and assume that the timing recovery is perfect, decision thresholds are optimized, and the receiver and transmitter are colocated.

Note that the discrete-time dispersive channel (f_k) contains a zero tap, a single precursor tap, and possibly multiple postcursor taps. Suppose that the channel contains m taps. Let s_j be an m-chip segment randomly taken from a DAPPM sequence, let $p(s_j)$ be the probability of occurrence of s_j, and let $I(s)$ be the receiver filter output (excluding noise) of
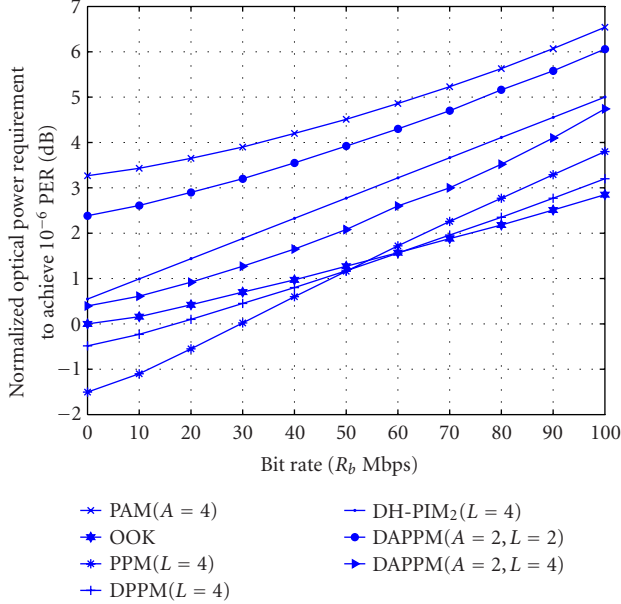
FIGURE 7: Average optical power requirement of PAM, OOK, PPM, DPPM, DH-PIM$_2$, and DAPPM versus bit rate R_b (Mbps) over a dispersive channel.

the next-to-last chip of s_j. The probability of chip error is

$$P_{ce} = \sum_j p(s_j)\epsilon(s_j), \qquad (17)$$

where

$$\epsilon(s_j) = \begin{cases} Q\left(\dfrac{(\theta_1 - I(s))P_c}{A\sqrt{N_0 W}}\right), & b_k = 0, \\[2ex] Q\left(\dfrac{(I(s) - \theta_i)P_c}{A\sqrt{N_0 W}}\right) + Q\left(\dfrac{(\theta_{i+1} - I(s))P_c}{A\sqrt{N_0 W}}\right), & b_k = i, \\[2ex] Q\left(\dfrac{(I(s) - \theta_A)P_c}{A\sqrt{N_0 W}}\right), & b_k = A. \end{cases}$$

$$(18)$$

Figure 7 shows the power required by DAPPM compared to the other modulation schemes to transmit an optical signal in a room with a 3.5 m height at different bit rates. Given the same number of bits/symbol ($M = 2$), DAPPM provides better power efficiency compared to PAM because the "off" chips between "on" chips of the symbols reduce the influence of ISI. Note that DH-PIM$_2$ requires less power than DAPPM.

Next, we compare the performance of DAPPM with PPM, DPPM, and DH-PIM$_2$ when the maximum length of a symbol is the same. DAPPM requires about 1 dB more transmit power than DPPM and 2 dB more than PPM when the bit rate is lower than 50 Mbps. When the bit rate is over 50 Mbps, the average optical power required with DAPPM is about 1.5 dB more than DPPM and 1 dB more than PPM. On the other hand, DH-PIM$_2$ requires more power than DAPPM. Intuitively, DAPPM has better bandwidth efficiency

and so is more susceptible to corruption by noise, but the influence of ISI is less than with PPM and DPPM at high bit rates. This is because the effects of ISI are alleviated by the longer symbol duration of DAPPM compared to that with PPM and DPPM. However, as shown in Figure 7, DAPPM has less power efficiency and requires more average optical power than PPM and DPPM.

5. MAXIMUM-LIKELIHOOD SEQUENCE DETECTION FOR DAPPM

5.1. Nondispersive channels

In [7], an MLSD was used for optimal soft decoding over a nondispersive channel when the symbol boundaries were not known prior to detection. Hence, we apply MLSD here to detect chip sequences of length D bits. MLSD essentially compares the received sequence with all possible D bit sequences. The chip sequence with the minimum Euclidean distance from the received sequence is chosen.

Given a DAPPM chip sequence, there are $D/\log 2(A \times L)$ "on" chips and the value of each "on" chip b_k is selected from $\{1, 2, \dots, A\}$. The error event which gives minimum distance error occurs when the amplitude of an "on" chip of the sequence is detected as other possible amplitude. Hence, the packet error rate of DAPPM with an MLSD receiver can be considered as the packet error rate of a PAM system with MLSD when the PAM symbol is $\{1, 2, \dots, A\}$ and each symbol is equally likely and independent. Moreover, the PAM packet length is equal to ($D/\log 2(A \times L)$). Then, the packet error rate of DAPPM with an MLSD receiver is given as

$$\text{PER} = \frac{2(A-1)}{A} \frac{D}{\log_2(A \times L)} Q\left\{\frac{0.5 P_c}{A\sqrt{N_0 W}}\right\}. \qquad (19)$$

Figure 8 illustrates the power required to achieve a 10^{-6} packet error rate for DAPPM with a hard-decision detection compared to that with an MLSD receiver. This shows that DAPPM with MLSD provides little performance improvement compared to hard-decision detection, especially when L is small.

5.2. Dispersive channels

Over a dispersive channel, we use a whitened matched filter at the front end of the receiver as shown in Figure 9a. This filter consists of a matched filter $r(t) = p(-t) * h(-t)$ followed by a sampler and a whitening filter w_k which whitens the noise and also eliminates the anticausal part of the ISI channel. Assuming perfect timing recovery, the discrete-time impulse response is

$$f_k = f(t)|_{t=kT_c} = \frac{P_c}{A} p(t) * h(t) * p(-t) * h(-t)|_{t=kT_c}, \qquad (20)$$

with ($2m + 1$) taps and a maximum point at f_0. Hence, the equivalent discrete-time system, $g_k = f_k * w_k$, has only ($m + 1$) postcursor taps. Consequently, the transmitted chip b_k is corrupted only by the past chips $\{b_{k-1}, \dots, b_{k-m}\}$.
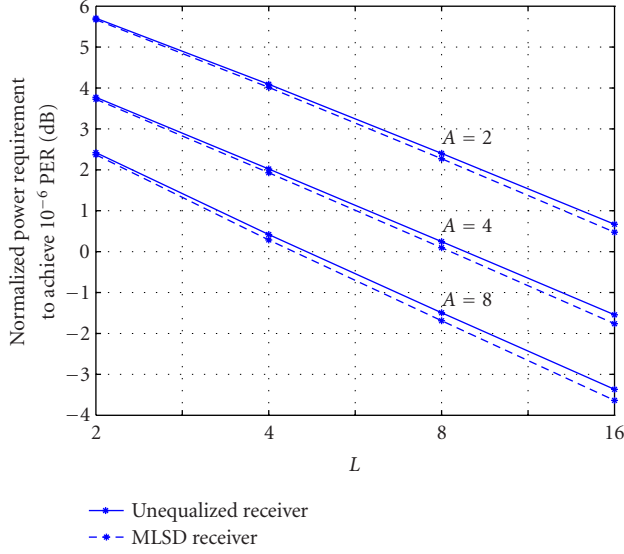
FIGURE 8: The required average power to achieve a 10^{-6} packet error rate for DAPPM with a hard-decision detection and an MLSD receiver over a nondispersive channel.
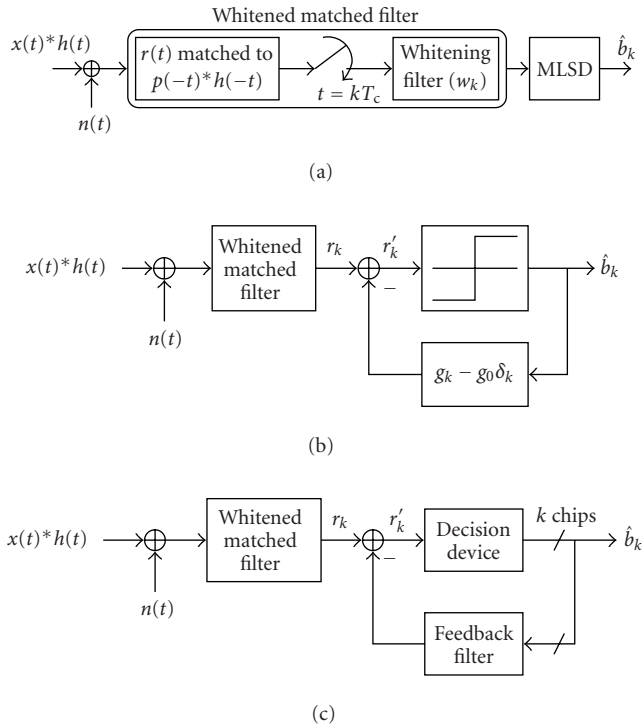

(a)

(b)

(c)

FIGURE 9: (a) Block diagram of a whitened-matched-filter MLSD receiver. (b) Block diagram of a chip-rate DFE receiver with a hard-decision detector. (c) Block diagram of a multichip-rate DFE receiver.

A method for determining the coefficients of a whitening filter w_k was proposed in [16]. First, we define $x(D) = x_0 + x_1 D + x_2 D^2 + \cdots$. Since $f(D)$ is a symmetric function and
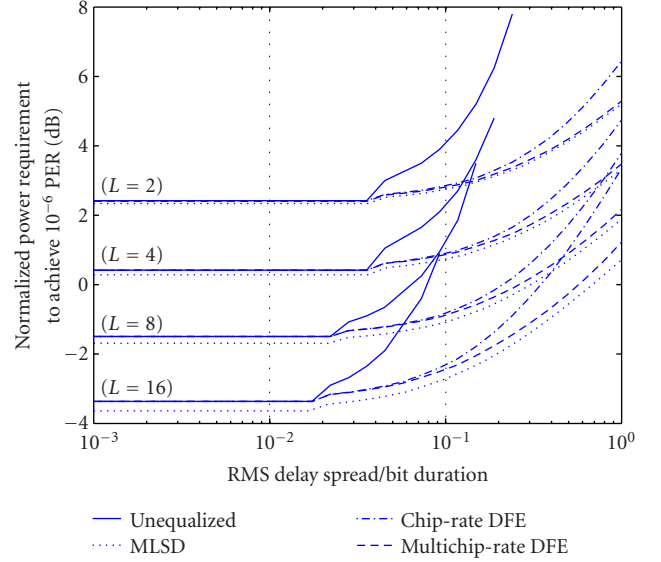

FIGURE 10: The required average power to achieve a 10^{-6} packet error rate for DAPPM with a hard-decision detection, an MLSD receiver, a chip-rate DFE receiver, and a multichip-rate DFE receiver over a dispersive channel, when $A = 2$.

has $(2m + 1)$ nonzero terms, it has $(2m)$ roots. $f(D)$ can be factored as

$$f(D) = W(D)W(D^{-1}), \qquad (21)$$

where $W(D)$ has m roots inside the unit circle and $W(D^{-1})$ has m roots which are the inverse-complex conjugate of the roots inside the unit circle. Hence, the whitening filter coefficients w_k are the coefficients of $(1/W(D^{-1}))$. When MLSD is used as a detector, the union bound packet error rate can be calculated as [17]

$$\text{PER} = \sum_{\mathbf{E}} P_{\mathbf{E}} Q\left(\frac{0.5 d_{\min} P_c}{A\sqrt{N_0 W}} \right), \qquad (22)$$

where the minimum Euclidean distance between two distinct chip sequences is

$$d_{\min}^2 = \min_{(\epsilon_k, 1 \le k \le K)} \sum_{i=1}^{m} \left| \sum_{k=1}^{K} \epsilon_k g_{h,m-k} \right|^2, \qquad (23)$$

and $P_{\mathbf{E}}$ represents the probability of sequence error $\mathbf{E} = \{\epsilon_1, \ldots, \epsilon_K\}$ when the minimum Euclidean distance is $\epsilon_k = b_k - \hat{b}_k$.

The performance using a whitened-matched-filter MLSD receiver in an ISI channel compared to other detectors is shown in Figure 10 for different ratios D_{rms}/T_b. Although the performance of the system with MLSD is not improved much when D_{rms}/T_b is low compared to the unequalized receiver, it is superior when D_{rms}/T_b is higher than about 0.09. Moreover, the power requirement of the system with MLSD is still at an acceptable level when D_{rms}/T_b is high.

6. ZERO-FORCING DECISION-FEEDBACK EQUALIZER FOR DAPPM

Although MLSD gives superior performance over a dispersive channel, it incurs a significant increase in complexity. In [6, 7], a zero-forcing decision-feedback equalizer (ZF-DFE) was used to obtain a good compromise between performance and complexity. In this section, we investigate the performance of a zero-forcing decision-feedback equalizer (ZF-DFE) with DAPPM in an ISI channel. As mentioned above, the discrete-time equivalent system, g_k, has only postcursor ISI. Therefore, the current chip has interference only from past chips. We utilize this property to mitigate the effects of ISI by feeding back past detected chips and subtracting the whitening-matched filter output from the past detected chips. The received chip $\hat{b}_k$ is estimated by a decision device. Shiu and Kahn [7] used two kinds of detectors: chip-by-chip detector and multiple-chip detector, which are discussed below.

6.1. Chip-rate DFE

The block diagram of a chip-rate DFE is given in Figure 9b. In this receiver, we use a hard-decision chip-by-chip detector. Thus, the transmitted chip b_k is determined using

$$\hat{b}_k = \begin{cases} 0 & \text{iff } r'_k < \dfrac{g_0}{2}, \\ i & \text{iff } (i-1) + \dfrac{g_0}{2} \le r'_k < i + \dfrac{g_0}{2}, \\ A & \text{iff } r'_k \ge (A-1) + \dfrac{g_0}{2}. \end{cases} \tag{24}$$

Assuming all past detected chips are correct, the packet error rate of this receiver is

$$\text{PER} = \left(p_0 + (2A - 1)p_A\right) Q\left(\frac{0.5 g_0 P_c}{A\sqrt{N_0 W}}\right). \tag{25}$$

6.2. Multichip-rate DFE

A trellis detector is employed as a decision device in multichip-rate DFE [7]. Instead of using only the information from the current WMF output, we also utilize information about future WMF outputs to estimate the transmitted chips. The block diagram of a multichip-rate DFE is given in Figure 9c. Suppose the decision device has access to the n most recent received chip samples $\{r'_i\}_0^{n-1}$. The postcursor ISI from $\{b_i\}$, $i < 0$, in $\{r'_i\}_0^{n-1}$ is completely removed by the ZF-DFE. The detector estimates the k transmitted chips $\{b_i\}_0^{k-1}$ by choosing a sequence of chips $\{b_i\}_0^{n-1}$ which minimizes $\sum_{i=0}^{n-1}(r'_i - \hat{b}_i * g_i)^2$. Let b^n denote $\{b_i\}_0^{n-1}$, and

$$d(b^n, c^n) = \left(\sum_{k=0}^{n-1} \left\{(b_k - c_k) * g_k\right\}^2\right)^{1/2}, \tag{26}$$

the Euclidean distance between the first n samples of $b^n * g_k$, and those of $c^n * g_k$ when the first k chips of c^n differ from

b^n. In the absence of error propagation, an upper bound on the packet error rate when $\{b_i\}_0^{k-1}$ is determined from the n most recent WMF outputs $\{r'_i\}_0^{n-1}$ is

$$\text{PER} \le \sum_{b^n} w(b^n) \cdot \sum_{c^n} Q\left(\frac{d(b^n, c^n)}{2\sqrt{N_0}}\right), \tag{27}$$

where $w(b^n)$ is the probability of b^n occurring.

The performance of DAPPM with a chip-rate DFE and a multichip-rate DFE ($n = 4$, $k = 1$) is given in Figure 10. This shows that using a DFE is superior to using an unequalized receiver, especially when D_{rms}/T_b is high. Moreover, the multichip-rate DFE performs very close to the MLSD receiver and requires much less complexity than MLSD. Thus, the multichip-rate DFE receiver is preferable in terms of both performance and complexity.

7. CONCLUSIONS

We introduced DAPPM and investigated its performance over an indoor wireless optical link. DAPPM provides several advantages. A DAPPM receiver is simple because it does not need symbol synchronization. We compared DAPPM with PPM, DPPM, and DH-PIM$_\alpha$ on the basis of required bandwidth, capacity, peak-to-average power ratio and required power over nondispersive and dispersive channels. It was shown that DAPPM requires less bandwidth when the number of amplitude levels is high. Furthermore, the capacity of DAPPM converges to $2A$ times and A times that of PPM and DPPM, respectively, when the number of bits/symbol increases. The capacity of DH-PIM$_2$ is about the same as DAPPM ($A = 2$). Hence, given the same symbol duration, DAPPM can provide a higher data rate than PPM, DPPM, and DH-PIM$_\alpha$. Also, DAPPM achieves a lower peak-to-average power ratio. However, it requires more average optical power than PPM, DPPM, and DH-PIM$_\alpha$ to achieve the same error probability.

Over a dispersive channel, given the same number of bits/symbol, DAPPM with an unequalized receiver provides better performance than PAM but it requires more power than DH-PIM$_2$. For the same maximum length, although DAPPM has better bandwidth efficiency, it requires more average optical power than PPM and DPPM but less power when compared to DH-PIM$_2$. When the rms delay spread is high compared to the bit duration, the packet error rate of DAPPM can be significantly improved by using MLSD, chip-rate DFE, or multichip-rate DFE, instead of a hard-decision receiver. Considering these receivers, the multichip-rate DFE is the most desirable in terms of both performance and complexity.

REFERENCES

[1] F. R. Gfeller and U. H. Bapst, "Wireless in-house data communication via diffuse infrared radiation," *Proc. IEEE*, vol. 67, no. 11, pp. 1474–1486, 1979.

[2] J. R. Barry, *Wireless Infrared Communications*, Kluwer Academic Publishers, Norwell, Mass, USA, 1994.

[3] J. B. Carruthers and J. M. Kahn, "Modeling of nondirected wireless infrared channels," *IEEE Trans. Commun.*, vol. 45, no. 10, pp. 1260–1268, 1997.

[4] Z. Ghassemlooy, A. R. Hayes, N. L. Seed, and E. D. Kaluarachchi, "Digital pulse interval modulation for optical communications," *IEEE Commun. Mag.*, vol. 36, no. 12, pp. 95–99, 1998.

[5] A. R. Hayes, Z. Ghassemlooy, N. L. Seed, and R. McLaughlin, "Baseline-wander effects on systems employing digital pulse-interval modulation," *IEE Proceedings-Optoelectronics*, vol. 147, no. 4, pp. 295–300, 2000.

[6] Z. Ghassemlooy, A. R. Hayes, and B. Wilson, "Reducing the effects of intersymbol interference in diffuse DPIM optical wireless communications," *IEE Proceedings-Optoelectronics*, vol. 150, no. 5, pp. 445–452, 2003.

[7] D.-S. Shiu and J. M. Kahn, "Differential pulse-position modulation for power-efficient optical communication," *IEEE Trans. Commun.*, vol. 47, no. 8, pp. 1201–1210, 1999.

[8] N. M. Aldibbiat, Z. Ghassemlooy, and R. McLaughlin, "Performance of dual header-pulse interval modulation (DH-PIM) for optical wireless communication systems," in *Proc. SPIE Optical Wireless Communications III*, vol. 4214 of *Proceedings of SPIE*, pp. 144–152, Boston, Mass, USA, February 2001.

[9] N. M. Aldibbiat, Z. Ghassemlooy, and R. McLaughlin, "Dual header pulse interval modulation for dispersive indoor optical wireless communication systems," *IEE Proceedings Circuits, Devices and Systems*, vol. 149, no. 3, pp. 187–192, 2002.

[10] S. Hranilovic and D. A. Johns, "A multilevel modulation scheme for high-speed wireless infrared communications," in *Proc. IEEE Int. Symp. Circuits and Systems (ISCAS '99)*, vol. 6, pp. 338–341, Orlando, Fla, USA, May–June 1999.

[11] R. Alves and A. Gameiro, "Trellis codes based on amplitude and position modulation for infrared WLANs," in *IEEE VTS 50th Vehicular Technology Conference (VTC '99)*, vol. 5, pp. 2934–2938, Amsterdam, Netherlands, September 1999.

[12] J. R. Barry, J. M. Kahn, W. J. Krause, E. A. Lee, and D. G. Messerschmitt, "Simulation of multipath impulse response for indoor wireless optical channels," *IEEE J. Select. Areas Commun.*, vol. 11, no. 3, pp. 367–379, 1993.

[13] J. G. Proakis, *Digital Communications*, McGraw-Hill, New York, NY, USA, 3rd edition, 1995.

[14] L. W. Couch, *Digital and Analog Communication Systems*, Prentice Hall, Englewood Cliffs, NJ, USA, 5th edition, 1997.

[15] Ir DA standard, "Fast serial infrared (FIR) physical layer link specification," *Infrared Data Association,* January 1994.

[16] G. D. Forney Jr., "Maximum-likelihood sequence estimation of digital sequences in the presence of intersymbol interference," *IEEE Trans. Inform. Theory*, vol. 18, no. 3, pp. 363–378, 1972.

[17] E. A. Lee and D. G. Messerschmitt, *Digital Communication*, Kluwer Academic Publishers, Norwell, Mass, USA, 2nd edition, 1994.

Ubolthip Sethakaset was born in Bangkok, Thailand, in 1976. She received the B. Eng. and M. Eng. degrees in electrical engineering from Kasetsart University in 1998 and 2000, respectively. She worked as a Research Assistant at Kasetsart University in 2001. Since 2002, she has been working toward the Ph.D. degree at the University of Victoria, Canada. Her research interests are in optical wireless communications, modulation schemes, and error-control coding.

T. Aaron Gulliver received the Ph.D. degree in electrical and computer engineering from the University of Victoria, Victoria, British Columbia, Canada, in 1989. From 1989 to 1991, he was employed as a Defence Scientist at the Defence Research Establishment Ottawa, Ottawa, Ontario, Canada. He has held academic positions at Carleton University, Ottawa, and the University of Canterbury, Christchurch, New Zealand. He joined the University of Victoria in 1999 and is a Professor in the Department of Electrical and Computer Engineering. He is a Senior Member of the IEEE and a Member of the Association of Professional Engineers of Ontario, Canada. In 2002, he became a Fellow of the Engineering Institute of Canada. His research interests include information theory and communication theory, algebraic coding theory, cryptography, construction of optimal codes, turbo codes, spread-spectrum communications, space-time coding, and ultra-wideband communications.